Fadil Al-Jaberi*, Melanie Fachet, Matthias Moeskes, Martin Skalej, and Christoph Hoeschen

# Optimization Techniques for Semi-Automated 3D Rigid Registration in Multimodal Image-Guided Deep Brain Stimulation

https://doi.org/10.1515/cdbme-2023-1089

**Abstract:** Multimodal image registration is vital in Deep Brain Stimulation (DBS) surgery. DBS treats movement disorders by implanting a neurostimulator device in the brain to deliver electrical impulses. Image registration between computed tomography (CT) and cone beam computed tomography (CBCT) involves fusing images with a specific field of view (FOV) to visualize individual electrode contacts. This contains important information about the location of segmented contacts that can reduce the time required for electrode programming. We performed a semi-automated multimodal image registration with different FOV between CT and CBCT images due to the tiny structures of segmented electrode contacts that necessitate high accuracy in the registration. In this work, we present an optimization workflow for multi-modal image registration using a combination of different similarity metrics, interpolators, and optimizers. Optimization-based rigid image registration (RIR) is a common method for registering images. The selection of appropriate interpolators and similarity metrics is crucial for the success of this optimization-based image registration process. We rely on quantitative measures to compare their performance. Registration was performed on CT and CBCT images for DBS datasets with an image registration algorithm written in Python using the Insight Segmentation and Registration Toolkit (ITK). Several combinations of similarity metrics and interpolators were used, including mean square difference (MSD), mutual information (MI), correlation and nearest neighbors (NN), linear (LI), and B-Spline (SPI), respectively. The combination of a correlation as similarity metric, B-Spline interpolation, and GD optimizer performs the best in optimizing the 3D RIR algorithm, enhancing the visualization of segmented electrode contacts. Patients undergoing DBS therapy may ultimately benefit from this.

***Corresponding author: Fadil Al-Jaberi, Melanie Fachet, Christoph Hoeschen,** Otto von Guericke University, Faculty of Electrical Engineering and Information Technology, Institute of Medical Technology, Chair of Medical Systems Technology. Corresponding author e-mail: fadil.al-jaberi@ovgu.de
**Matthias Moeskes,** Otto von Guericke University, Medical Faculty, Institute of Biometry and Medical Informatics.
**Martin Skalej,** Martin Luther University Halle-Wittenberg, Medical Faculty, Neuroradiology.

**Keywords:** Image Registration, Cone Beam Computed Tomography, Computed Tomography, Similarity Metric, Semi-automated Registration, Deep Brain Stimulation.

## 1 Introduction

Deep Brain Stimulation (DBS) is a medical treatment increasingly used to treat movement disorders such as Parkinson's disease, dystonia, and tremors [1], as well as psychiatric conditions such as treatment-resistant depression [2]. The procedure involves placing electrodes inside specific regions of the brain to alter their electrical activity in a controlled manner. Accurate placement and programming of the DBS device require knowledge of the stimulation target and electrode location. Typical clinical procedures involve the use of computed tomography (CT) imaging before surgery to aid in stereotaxic guidance and after surgery to check for bleeding and ensure proper electrode orientation. Intraoperative X-ray imaging is also used to visualize the tiny orientation markers of the electrode [3][4]. To visualize the target region, magnetic resonance imaging (MRI) can be used. The subthalamic nucleus, which is the most significant deep brain target in Parkinson's disease, can be visualized through MRI. In addition to CT and MRI, Cone Beam Computed Tomography (CBCT) with a specific field of view (FOV) is employed in DBS procedures. CBCT protocols customized for implant placement are preferred because they offer higher spatial resolution and less interference from scatter and metal artifacts compared to multislice CT. To align the CBCT image which has a specific FOV with other imaging modalities such as CT and MRI, a semi-automated registration technique is performed. This registration allows for better visualization of the target region. The combination of interpolation, similarity metrics, and optimization methods plays a crucial role in achieving accurate registrations. Rigid image registration (RIR) is a common technique used to align images, and optimization methods are employed to estimate the most appropriate transformation. However, undersampled or oversampled images can lead to registration errors [5]. There have been several studies looking at the effect of interpolation on image registration by various authors [6][7]. J. P. Pluim et al. [6] studied the effects of interpolation

methods on speed and artifacts in accuracy of image registration. In their study, A. P. Mahmoudzadeh et al. [7] assessed eight different interpolation methods and examined how the cost functions influenced the optimization of fully automatic image registration for 3D spoiled gradient MRI. The evaluation was complemented by qualitative assessments using MRI scans and joint histogram analysis. B. Handa et al. [8] investigated the efficiency of 3D RIR in radiotherapy using various combinations of interpolators and similarity metrics. In their study, B. Handa et al. [8] utilized multimodal imaging with CT and CBCT scans to examine the pelvis. Both images had the same pixel spacing and matrix size, indicating they had the same FOV. However, in our dataset, we are dealing with brain images with implanted DBS electrodes and the images have different pixel spacing. Specifically, the CBCT image has a narrower FOV. Choosing the right interpolator and similarity metric can improve registration accuracy. This paper analyzes and compares semi-automated image registration utilizing different combinations of interpolators and similarity metrics.

# 2 Material and Methods

## I. Multimodal Image Data Acquisition

Our dataset consists of retrospective data from patients who underwent surgery to have bilateral DBS-lead implantation. While CT was performed right after surgery a highly resolved CBCT was acquired within the first week after surgery. On average, there was a 4.5-day time difference between the two examinations. The ArtisQ multipurpose x-ray system with syngo microDyna-CT was used for CBCT acquisition and a Somatom Definition AS+ for CT (both Siemens Healthineers, Germany). The acquisition settings for CBCT included anode voltage of 116-119 kV, tube current ranging from 258-274 mA, and a pixel matrix of size $512\times512\times497$ with an isotropic voxel size of $0.1965\times0.1965\times0.1965$ mm after 3D-image reconstruction. The conventional CT was performed with an anode voltage of 120 kV and tube current of 370 mA. It provided 197(-253) slices with an image size of $512\times512$, and the voxel sizes ranged from $0.4(-0.6)\times0.4(-0.6)\times0.75$ mm. The voxel sizes were adjusted by a radiological technician based on the FOV.

## II. Semi-automated Registration with ITK

This paper relies on the open-source software Insight Segmentation and Registration Toolkit (ITK) and programming language Python. ITK is a widely used research toolkit for medical imaging, particularly for segmenting and registering medical images [9][10]. To execute our workflow, we used a 64-bit Windows 10 Pro operating system with an Intel Core i7-11700 processor running at 2.5 GHz and 32 GB RAM. Our method is a semi-automated registration workflow for multimodal images based on ITK. The used images include CT images and CBCT images with a narrow FOV, which depict the region of interest for DBS electrodes. The registration consists of two stages: the initial transformation and the final transformation. In the initial transformation stage, corresponding points are selected via user input based on anatomical landmarks. This is done after setting the appropriate windowing for both images, allowing the user a suitable window for identifying anatomical landmarks. The initial transformation is crucial for the final transformation, where shortening the runtime and increasing the accuracy of registration convergence.

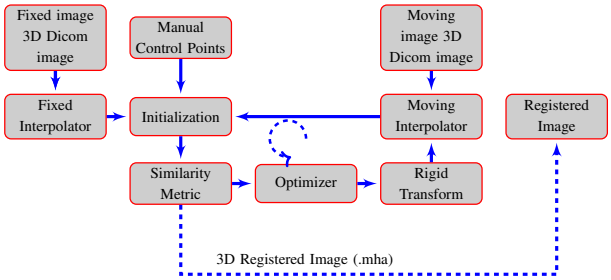


**Fig. 1:** Framework for semi-automated RIR based on ITK.

The final transformation of the registration depends on the initial transformation, and also involves the following components:

**A. Optimizers:** The ITK registration framework offers support for several optimizer types. In this work, we utilized the optimizer options of Variations on Gradient Descent (GD), and Regular Step Gradient Descent (RSGD).

**B. Similarity metrics:** One of the common similarity metrics is Mattes Mutual Information (MMI), which was employed in this study. This metric measures the mutual information between the fixed and moving images and is widely used in medical image registration tasks.

**C. Interpolators:** In our investigation to identify the most suitable interpolators, we tested three different types: Linear (LI), Nearest Neighbor (NN), and B-Spline (SPI) interpolation. These interpolators are commonly used in medical image processing and were chosen based on their effectiveness in preserving image quality and accuracy during registration.

Figure 1: It illustrates the registration components used in this type of registration. It also shows the manual control points used by the user to initialize images using the corresponding points between CT and CBCT images.

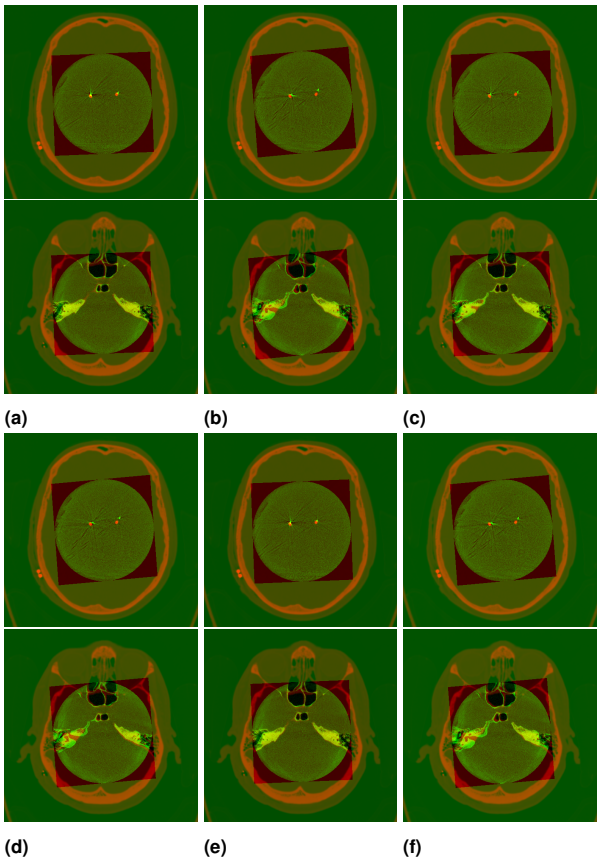


**Fig. 2:** Image fusion results for different combinations of similarity metrics, interpolators and optimizers, where each subfigure represents one combination, two images to show the anatomical, and electrodes regions: (a) MMI, LI, GD (b) MMI, LI, RSGD (c) MMI, NNI, GD, (d) MMI, NNI, RSGD (e) MMI, SPI, GD, and (f) MMI, SPI, RSGD.

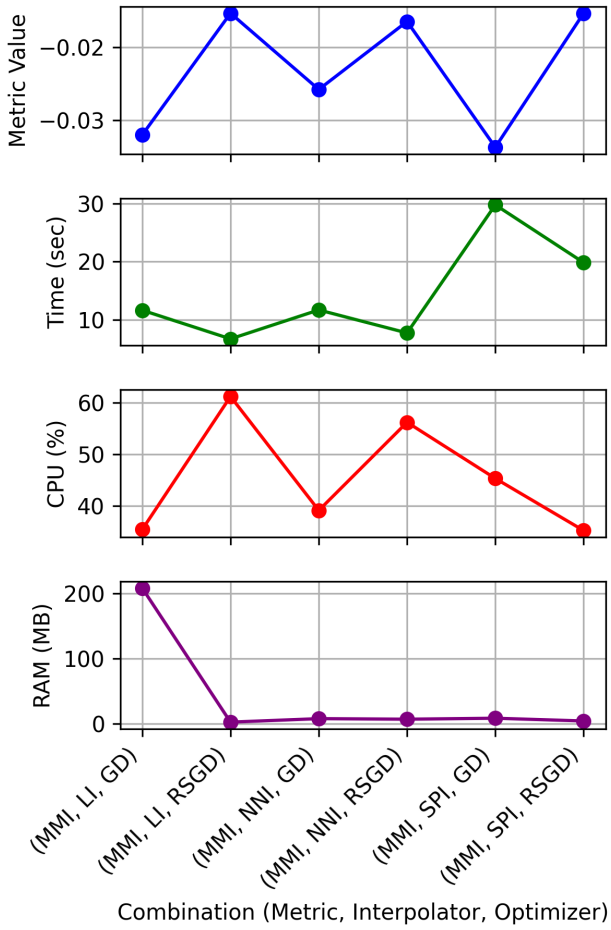


**Fig. 3:** Comparison of similarity metric, interpolation, and optimizers. The top subfigure shows the final metric values for each combination of similarity metric, interpolation, and optimizer, allowing for easy comparison of the best-performing combinations, where the larger the negative values, the more accurate the image registration will be. The bottom subfigure displays the time consumed, CPU usage, and RAM usage for each combination, providing valuable insight into the computational demands of each group of combinations.

# 3 Results

Table 1 presents the quantitative evaluation results in terms of the final metric value. Moreover, Figure 3 provides further insights into the final metric value for each combination of similarity metric, interpolator, and optimizer, along with their respective CPU and memory usage and computation time. Additionally, Figure 2 illustrates two slices of the registered images that highlight the alignment of anatomical structures and electrodes for each combination of similarity metric, interpolator, and optimizer, where Figure 2e shows the best anatomical alignment using GD optimizer, B-spline interpolation and correlation as similarity metric.

**Tab. 1:** Comparing RIR accuracy based on ITK-based algorithms with various combinations of similarity metrics, interpolators, and optimizers based on final metric values of optimizers GD, and RSGD.

| Similarity Metric | Interpolator | GD | RSGD |
|---|---|---|---|
| Mutual Information | Linear | -0.032 | -0.015 |
| Mutual Information | Nearest neighbor | -0.025 | -0.016 |
| Mutual Information | B-spline | -0.033 | -0.015 |
| Mean square | Linear | 483971 | 433743 |
| Mean square | Nearest neighbor | 524906 | 513133 |
| Mean square | B-spline | 506171 | 502352 |
| Correlation | Linear | -0.020 | -0.026 |
| Correlation | Nearest neighbor | -0.027 | -0.020 |
| Correlation | B-spline | -0.043 | -0.023 |

# 4 Discussion

In the past few decades, several techniques for image registration have been developed for a wide range of datasets [11][5][12][13]. In this study, the medical imaging datasets for the brain were used in comparison with the pelvic images. There are some publications that describe fully automated 3D RIR of the pelvic region of the body. However, there are a few that report semi-automated RIR of 3D image datasets [14][15][5]. There have been several studies looking at the effect of interpolation on imaging registration using CT and MRI images with the same pixel spacing by various authors [6][7]. In this study, the first similarity metrics, interpolators, and optimizers were utilized to increase the accuracy of semi-automated 3D RIR in the DBS images dataset. Second CBCT and CT images were utilized instead of CT and MRI images. This is because, in DBS surgery with the narrow FOV of CBCT images, CBCT images are provided with high resolution. This will help us visualize the segmented contacts in each electrode lead. In terms of quantitative metrics using the final metric value, the registration algorithm efficiency was evaluated using a different combination of interpolators and similarity metrics. It is observed that the final metric value of the interpolator is affected by combinations of similarity metrics and optimizers. This research will be extended to include fully automated RIR between CT and CBCT images with a narrow FOV.

# 5 Conclusions

In this study, a combination of a correlation as similarity metric, B-Spline interpolator, and GD optimizer showed the best performance to optimize the 3D RIR algorithm, in terms of registration accuracy, but in terms of CPU, memory, and time consumption, they are pretty close. This approach was found to result in better efficiency in image registration when compared to other combinations of interpolators and optimizers. The results were obtained through the use of quantitative measures, which shows congruence with the qualitative assessment, the results are visualized in Figure 2. Even a tiny improvement in CT and CBCT image registration can have a significant impact on the visualization of the segmented contacts of electrodes in DBS. This can in turn lead to better outcomes for patients undergoing DBS therapy.

**Acknowledgment:** This work was partially supported by Deutscher Akademischer Austauschdienst (DAAD) under funding programme research grants - Doctoral programmes in Germany (57440921).

# References

[1] A. M. Lozano, N. Lipsman, H. Bergman, P. Brown, S. Chabardes, J. W. Chang, K. Matthews, C. C. McIntyre, T. E. Schlaepfer, M. Schulder, *et al.*, "Deep brain stimulation: current challenges and future directions," *Nature Reviews Neurology*, vol. 15, no. 3, pp. 148–160, 2019.

[2] J. Kuhn, T. O. Gründler, D. Lenartz, V. Sturm, J. Klosterkötter, and W. Huff, "Deep brain stimulation for psychiatric disorders," *Deutsches Arzteblatt International*, vol. 107, no. 7, p. 105, 2010.

[3] J. M. Schmidt, L. Buentjen, J. Kaufmann, D. Gruber, H. Treuer, A. Haghikia, and J. Voges, "Deviation of the orientation angle of directional deep brain stimulation leads quantified by intraoperative stereotactic x-ray imaging," *Neurosurgical Review*, pp. 1–8, 2022.

[4] N. J. Vickers, "Animal communication: when i'm calling you, will you answer too?," *Current biology*, vol. 27, no. 14, pp. R713–R715, 2017.

[5] R. Bhagalia, J. A. Fessler, and B. Kim, "Gradient based image registration using importance sampling," in *3rd IEEE International Symposium on Biomedical Imaging: Nano to Macro, 2006.*, pp. 446–449, IEEE, 2006.

[6] J. P. Pluim, J. A. Maintz, and M. A. Viergever, "Interpolation artefacts in mutual information-based image registration," *Computer vision and image understanding*, vol. 77, no. 2, pp. 211–232, 2000.

[7] A. P. Mahmoudzadeh and N. H. Kashou, "Evaluation of interpolation effects on upsampling and accuracy of cost functions-based optimized automatic image registration," *Journal of Biomedical Imaging*, vol. 2013, pp. 16–16, 2013.

[8] B. Handa, G. Singh, R. Kamal, A. S. Oinam, and V. Kumar, "Evaluation method for the optimization of 3d rigid image registration on multimodal image datasets," *Volume-9 Issue-1*, p. 234, 2019.

[9] Z. Yaniv, B. C. Lowekamp, H. J. Johnson, and R. Beare, "Simpleitk image-analysis notebooks: a collaborative environment for education and reproducible research," *Journal of digital imaging*, vol. 31, no. 3, pp. 290–303, 2018.

[10] R. Beare, B. Lowekamp, and Z. Yaniv, "Image segmentation, registration and characterization in r with simpleitk," *Journal of statistical software*, vol. 86, 2018.

[11] A. Sotiras, C. Davatzikos, and N. Paragios, "Deformable medical image registration: A survey," *IEEE transactions on medical imaging*, vol. 32, no. 7, pp. 1153–1190, 2013.

[12] X. Wang, L. Li, C. Hu, J. Qiu, Z. Xu, and Y. Feng, "A comparative study of three ct and mri registration algorithms in nasopharyngeal carcinoma," *Journal of applied clinical medical physics*, vol. 10, no. 2, pp. 3–10, 2009.

[13] W. Wein, B. Röper, and N. Navab, "2d/3d registration based on volume gradients," in *Medical Imaging 2005: Image Processing*, vol. 5747, pp. 144–150, SPIE, 2005.

[14] S. Oh and S. Kim, "Deformable image registration in radiation therapy," *Radiation Oncology Journal*, vol. 235, no. 2, pp. 101–111, 2017.

[15] M. V. Wyawahare, P. M. Patil, H. K. Abhyankar, *et al.*, "Image registration techniques: an overview," *International Journal of Signal Processing, Image Processing and Pattern Recognition*, vol. 2, no. 3, pp. 11–28, 2009.